Iron deficiency induced changes in Fe homeostasis and 14-3-3 interactomics of Arabidopsis thaliana

Jing Gao
Chinese Academy of Agricultural Sciences
Paula J. M. Kleeff
Vrije Universiteit Amsterdam
Ka Wan Li
Vrije Universiteit Amsterdam
Albertus H. Boer (ahdeboer54@gmail.com)
Vrije Universiteit Amsterdam

Research Article

Keywords: Arabidopsis thaliana, ion homeostasis, Fe deficiency, 14-3-3 proteins, interactome

Posted Date: April 26th, 2021

DOI: https://doi.org/10.21203/rs.3.rs-445322/v1

Version of Record: A version of this preprint was published at Scientific Reports on July 30th, 2021. See the published version at https://doi.org/10.1038/s41598-021-94908-9.

Iron deficiency induced changes in Fe homeostasis and 14-3-3 interactomics of *Arabidopsis thaliana*

Jing Gao[1, 2], Paula J. M. van Kleeff[2, 4], Ka Wan Li[3], and Albertus H. de Boer[2]*

[1]Institute of Apicultural Research, Chinese Academy of Agricultural Sciences, 100093, Beijing, China

[2]Department of Structural Biology, Faculty of Earth and Life Sciences, Vrije Universiteit Amsterdam, De Boelelaan 1085, 1081 HV, Amsterdam, the Netherlands

[3]Department of Molecular and Cellular Neurobiology, Faculty of Earth and Life Sciences, Center for Neurogenomics and Cognitive Research, Vrije Universiteit Amsterdam, De Boelelaan 1085, 1081 HV, Amsterdam, the Netherlands

[4]Swammerdam Institute for Life Sciences, Department of Plant Physiology, University of Amsterdam, Kruislaan 318, 1098 SM, Amsterdam, the Netherlands

*** Correspondence:**

Albertus H. de Boer

ahdeboer54@gmail.com

Keywords: *Arabidopsis thaliana*, ion homeostasis, Fe deficiency, 14-3-3 proteins, interactome.

Abstract

Members of 14-3-3 protein family are involved in the proper operation of Fe acquisition mechanisms at physiological and gene expression levels in *Arabidopsis thaliana*. To more directly and effectively observe whether members of 14-3-3 non-epsilon group have a function in Fe-deficiency adaptation, three higher order quadruple KOs,

kappa/lambda/phi/chi (*klpc*), kappa/lambda/upsilon/nu(*klu*n), and upsilon/nu/phi/chi (*unpc*) were generated and applied for physiological analysis in this study. The mutant plants that combine *kl* with *un* (*klun*) or *kl* with *pc* (*klpc*) mutations showed a better Fe uptake than Wt plants at low medium Fe, while this phenotype was absent in *unpc* mutant. The higher Fe uptake by *klun* correlated with a higher Fe-deficiency induced expression of selected Fe-related genes. The dynamics of 14-3-3-client interactions analysis showed that a subset of 27 proteins differentially interacted with 14-3-3 in roots caused by Fe deficiency. Many of these Fe responsive proteins have a role in glycolysis and TCA cycle, the FoF1-synthase and in the cysteine/methionine synthesis. Also, the 14-3-3 interactome of the *klun* roots showed significant differences with that of Wt roots under Fe sufficient conditions, where most of these differential binding proteins showed enhanced binding in the *klun* mutant. Nevertheless, a clear explanation for the observed phenotypes awaits a more detailed analysis of the functional aspects of 14-3-3 binding to the target proteins identified in this study.

Introduction

Iron deficiency may lead to decreases in vegetative growth and quality losses, also known as "lime-induced chlorosis". Although iron is the fourth most abundant element in the earth's crust, it is mainly in the Fe^{3+} form and not soluble in soils. To cope with low Fe availability, plants have evolved two distinct strategies to enhance the uptake of the poorly soluble iron compounds from soil. One of them, known as the "reduction strategy" (Strategy I) involves a number of key genes, e.g. *FRO2* and *IRT1*, which co-regulate the root high-affinity iron uptake system [1,2].

14-3-3 proteins are a class of molecular chaperones that bind to and thereby influence the function of phosphorylated proteins [3]. The members of the 14-3-3 proteins, known as important regulators in osmotic stress and salt stress responses in plants, were also found as a key regulator required for the proper operation of Fe acquisition mechanisms at physiological and gene expression levels in *Arabidopsis thaliana* [4]. Loss-of-function

of *grf11* (14-3-3 chi) resulted in failure of rhizosphere acidification and ferric chelate reductase (FCR) induction, and thus decreased Fe uptake. Moreover, expression of *IRT1*, *FRO2*, and *AHA2*, were repressed in the *grf11* mutant both under Fe-deficient and under Fe-sufficient conditions. Recently, Singh et al. have demonstrated that a key factor, NON-RESPONSE TO Fe-DEFICIENCY2 (NRF2)/ EARLY FLOWERING8 (ELF8), controls Fe- deficiency response via GRF11 by the activation of histone H3 lysine 4 trimethylation (H3K4me3) in plant roots[5]. In detergent-resistant membranes (DRMs) of sugar beet roots, the Fe deficiency induced a decrease in abundance of six 14-3-3 like proteins, which would be in line with the decreases in relative abundance of an important number of kinases, e.g. CDPK (calcium dependent protein kinase). It is tempting to speculate that Fe deficiency induces the signaling cascades during phosphorylation processes at the plasma membrane level which are involved in interactions with 14-3-3 proteins [6].

Growing evidence demonstrates that 14-3-3 proteins play different affinities in the interaction with specific target proteins, what suggests that the large number of 14-3-3 isoforms in plants may reflect functional specificity [7]. It has been proposed that the interaction specificity of certain 14-3-3 isoforms may involve the outer surface of 14-3-3, which shows variation between isoforms [8]. For instance, 14-3-3 isoforms from tobacco (*Nicotiana tabacum* L.) present a difference in affinity towards Sucrose-6-phosphate synthase (SPS) in the yeast two-hybrid system [9]. Compared to 14-3-3 isoforms belonging to the epsilon group，non-epsilon 14-3-3 isoforms were more active in the interaction and activation of H^+-ATPase [10]. Furthermore, a large scale proteomics investigation showed that 14-3-3 target proteins bound differentially to 14-3-3 isoforms chi and epsilon during *Arabidopsis* seed development [7]. Quantitative proteomics [11,12], as well as a phosphoproteomics profile [13] of plants exposed to Fe deficiency, show that some putative 14-3-3 targets, such as fructose-bisphosphate aldolase, cytosolic alkaline invertase 1 (CINV1), nitrate reductase (NR) and H^+-ATPase were subject to change by Fe deficiency in *Arabidopsis* roots.

Since 14-3-3 proteins regulate so many proteins with a function in Fe acquisition process, it is to be expected that knock-out mutations in 14-3-3 genes will result in Fe-deficiency stress related phenotypes. However, the *Arabidopsis* genome contains thirteen expressed 14-3-3 genes and redundancy may exist between these isoforms [14,15]. According to amino acid sequence data and gene structure, the 14-3-3 members break into two major branches, the epsilon group and the non-epsilon group. The epsilon members are found in all organisms and are thought to be involved in basal eukaryotic 14-3-3 functions, while the non-epsilon group may be responsible for organism-specific regulatory aspects [14]. Both phosphate(P) and nitrate(N) deprivation cause isoform-specific and organ specific 14-3-3 transcript alterations. For instance, under phosphate efficiency, epsilon-group members are more affected compared to non-epsilon group members. Transcripts of *PSI*, *MU*, *OMICRON* and *PI* are decreased while *CHI*, *LAMBDA* and *KAPPA* are unchanged [16]. *KAPPA* expression is increased in leaves after K^+-deprivation but not in roots and the expression of *CHI* did not change under nutrient deprivation [17]. Van Kleeff et al. conducted a series of growth experiments with higher order *Arabidopsis* 14-3-3 mutants and showed gene specificity and functional redundancy among non-epsilon group members in primary root elongation under control and abiotic stress conditions [18]. Previous studies have demonstrated that root growth, hormone sensitivity and more specifically the activation of a neutral cytosolic invertase, indeed showed both specificity and redundancy amongst 14-3-3 non-epsilon group members, *kappa*, *lambda*, *phi*, *chi*, *upsilon* and *nu* [18]. As other 14-3-3 member may take over the role of the mutated gene, a large number of 14-3-3 single mutant plants may lack a phenotype [18-20]. To investigate whether members of the non-epsilon group have a function in Fe-deficiency adaptation, higher order mutants must be obtained by combining the respective single mutant. Three higher order quadruple KOs, *kappa*/*lambda*/*phi*/*chi* (*klpc*), *kappa*/*lambda*/*upsilon*/*nu*(*klun*), and *upsilon*/*nu*/*phi*/*chi* (*unpc*) were generated and applied for physiological analysis in this study.

In this work, we comprehensively investigate plant growth, Fe uptake, gene expression and quantitative 14-3-3 interactomics to define the biological role of a sub-class of 14-3-3 (non-epsilon group) in the response of *A. thaliana* wild-type and 14-3-3 mutant plants to Fe deficiency.

RESULTS

Physiological responses of the 14-3-3qKO lines to Fe deficiency. To investigate whether members of the non-epsilon group have a function in Fe-deficiency adaptation, three 14-3-3 quadruple KOs, *kappa*/*lambda*/*phi*/*chi* (*klpc*), *kappa*/*lambda*/*upsilon*/*nu* (*klun*), and *upsilon*/*nu*/*phi*/*chi* (*unpc*), were used in this study. The quadruple mutants were generated by crossing two double mutants: *kl*pc*, *kl*un* and *un*pc*. T-DNA insertions were monitored using PCR and the mutants were scored on full length 14-3-3 transcripts (for details see [18]). To measure the effect of Fe deficiency on biomass production, wild-type (Wt) and 14-3-3 qKO plants were grown on hydroponics (½ strength Hoagland)with 20 µM Fe-EDTA for 2 weeks and then transferred to a medium with different Fe concentrations (0 µM, 2 µM, 5 µM and 20 µM) for 12 days before harvest. All genotypes maintained fresh weight production when grown at 5 µM Fe as compared to the control plants (20 µM Fe) (Figure 1). All genotypes present iron chlorosis when grown at 0 µM and 2 µM Fe (Figure S1). At 2 µM Fe, *klpc* showed a significant growth reduction of both shoot and root and at 0 µM Fe all genotypes produced less biomass, whereat *unpc* showed the strongest growth reduction of shoot and root growth; 40 and 33% resp. All genotypes grown at 0 µM Fe also showed Fe-deficiency symptoms in the young leaves, which were pale green or yellow.

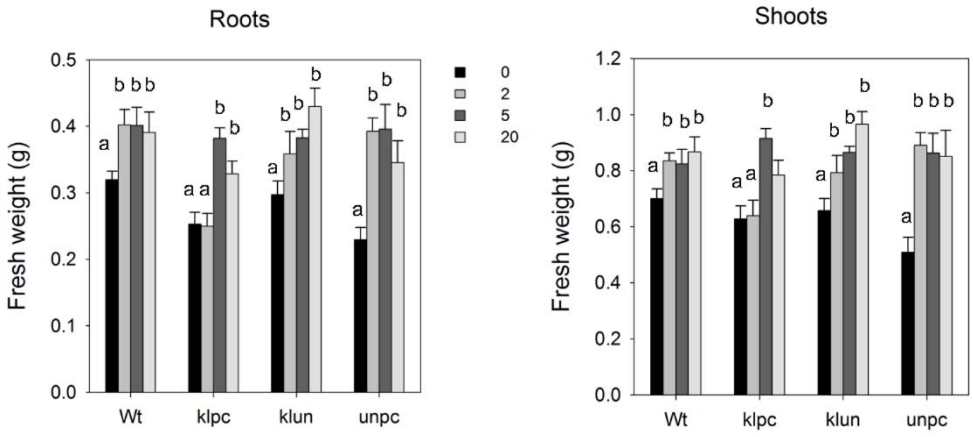

Figure 1. Growth performance of Wt and 14-3-3 qKOs under different Fe deficiency treatment. After two weeks of growth on ½ strength Hoagland solution, plants were grown for an additional 12 days at 0, 2, 5 and 20 μM (= sufficient) Fe. Fresh weight of roots (A), shoots (B) were measured from Wt and 14-3-3 qKOs plants. Each bar represents the mean of 10 biological replicates. The line above each bar is the SE. Means with different superscripts are significantly different at $P<0.05$, by two-way ANOVA followed by Bonferroni's post hoc test.

In the same plants as described above, the Fe contents of dry shoot and root material were measured. Overall, the Fe contents were decreased two- to three-fold in the shoot of Fe-starved plants (Figure 2) and the Fe content of Wt shoot was overall lower than that of the mutants. Notably, *klun* plants had significantly more Fe in their shoots than Wt plants at 0, 2 and 5 μM Fe-EDTA. The Fe content of roots, grown at ½ strength Hoagland with 20 μM Fe was more than 23-fold higher than that in the corresponding shoots (Figure 2A and 2B). Another difference between roots and shoots is that growth under Fe-starvation conditions induces a much stronger decrease in root Fe than in the shoot Fe content: up to 25-fold reduction. The comparison between the genotypes shows that also in the roots, *klun* has a significantly higher Fe content at 0 and 2 μM Fe as compared to Wt: at 0 μM the difference is 2-fold. As a measure of Iron-Utilization Efficiency (IUE) we calculated the ratio between fresh weight and the Fe content of the shoot and root (Figure 2C and D). Strikingly, the IUE of Wt shoot and root at 0 μM Fe is much higher than that of the 14-3-3 mutants, what points to a more efficient use of available Fe in the Wt plants. Moreover, the root IUE of *klun* at 0 and 2 μM and that of *klpc* at 2 μM Fe is significantly lower than that of the other genotypes (Figure 2D). Thus, the uptake of Fe by some mutants is clearly better than that of Wt, whereas the use of Fe by Wt plants to sustain growth is better at the lowest Fe concentrations.

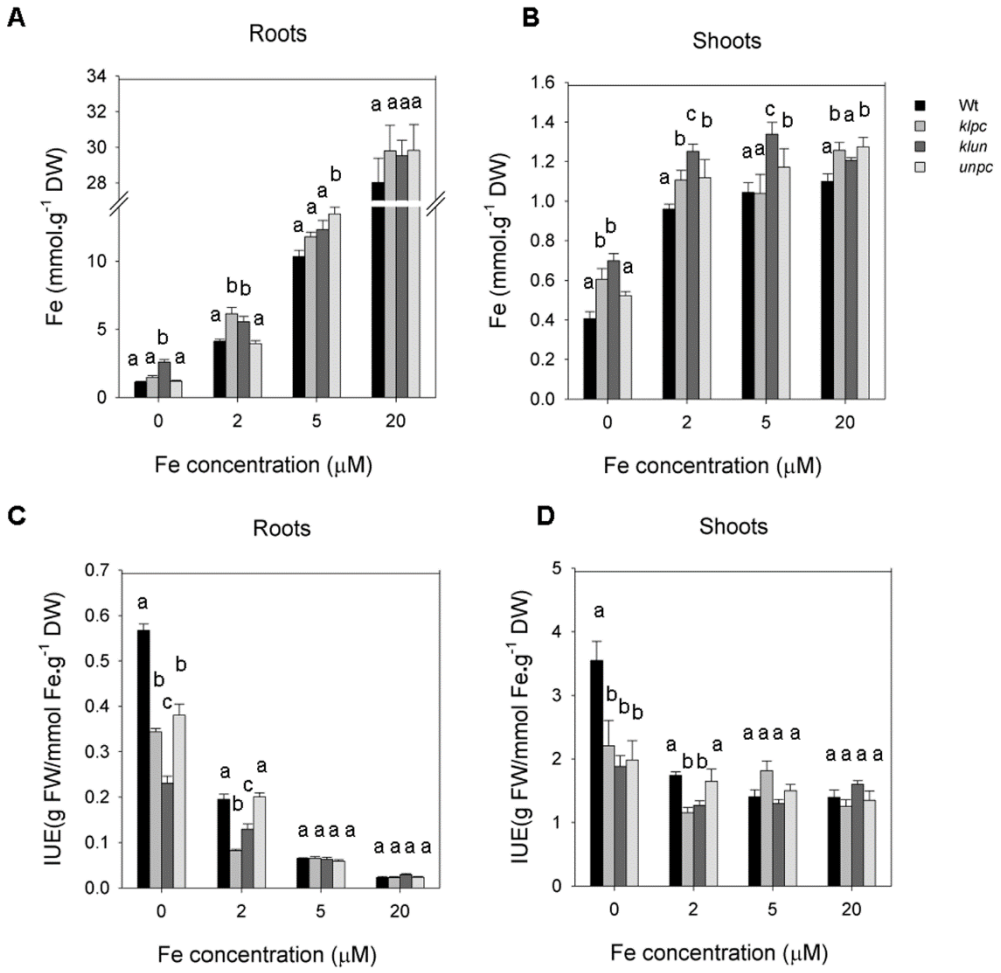

154

155 **Figure 2. Fe content of shoots and roots of WT and 14-3-3 qKOs plants.** After two
156 weeks of growth on ½ strength Hoagland solution, plants were grown for an additional 12
157 days at 0, 2, 5 and 20 μM (= sufficient) Fe. Shoots and roots were harvested, weighed and
158 pooled per two for the Fe-determination. A and B, Fe-content of roots and shoots; C and D,
159 Iron Use Efficiency (IUE) of roots and shoots. Each bar represents a mean of observations
160 in 5 biological replicates, ± SE. Averages with different superscripts are significantly
161 different at $P<0.05$, by two-way ANOVA followed by Bonferroni's post hoc test.

162 **Expression of Fe deficiency-induced genes is enhanced in the klun mutant plant**.
163 *Arabidopsis* follows Strategy I for iron acquisition, involving rhizosphere acidification
164 by plasma membrane H^+-ATPases (AHA2), reduction of Fe(III) to Fe(II) performed by
165 FRO2 and import of Fe(II) by the Fe transporter IRT1 [21,22]. Under Fe deficiency, high-
166 level expression of the genes encoding the abovementioned proteins is controlled by
167 the bHLH transcription factor FIT, where the induction of FIT expression is dependent
168 on the 14-3-3Omicron protein (Figure 3) [4]. Whereas physiological changes are only
169 manifest after long term Fe starvation, gene expression responds within 24 h [21,23].
170 Therefore, we measured Fe deficiency-induced expression of 14-3-3Omicron, FIT,
171 FRO2, IRT1 and AHA2 in roots of Wt and 14-3-3 qKOs after 24 h by quantitative real-

time PCR (qPCR) (Figure 3). In Wt plants, the 24 h Fe starvation induced a 2-(AHA2) to 18-fold (14-3-3Omicron) increase in transcript of all 5 genes. Under Fe sufficient conditions,*klpc*mutants showed significantly higher expression of FIT, GRF11, and FRO as compared to Wt, but these differences disappeared when the plants were Fe starved. The most obvious effect of Fe deficiency on gene expression is shown by the *klun* plants: under Fe sufficient conditions the expression of all genes is comparable to that in Wt, but under Fe starvation, the expression of the 5 genes is much higher than in Wt plants (Figure 3). This suggests that somehow the 14-3-3*Kappa/Lambda/Upsilon/Nu* proteins act as negative regulators of gene expression when the plants are Fe-starved.

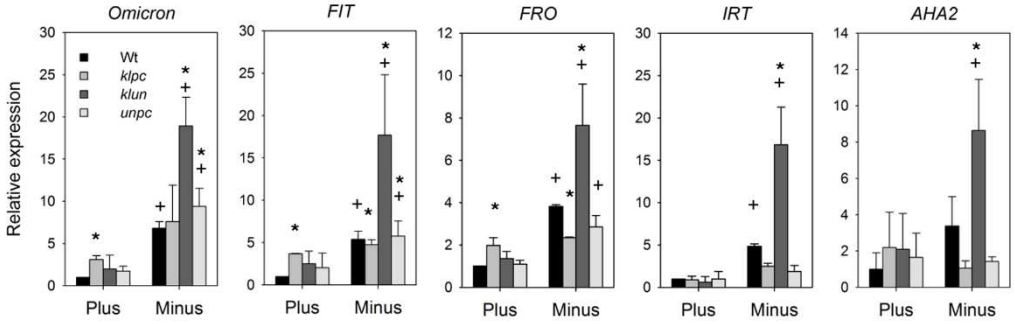

Figure 3. Expression analysis of 14-3-3 Omicron, FIT, FRO, IRT and AHA2 in Wt and 14-3-3 qKO lines grown with (plus) and without (minus) Fe. A. thaliana seedlings were grown in +Fe medium for 22 days and then transferred to nutrient medium with or without Fe for 24 hours. Expression levels were normalized to ubiquitin 10 (UBQ10) and then to the value of each gene from the Wt under Fe-sufficient conditions. Values are means ± SD (n = 3). +, significant change vs +Fe； *, significant change vs WT + Fe at P <0.05 (one-way-ANOVA).

Quantitative affinity-purification mass spectrometry analysis of the 14-3-3 interactome of Wt roots as affected by Fe deficiency. In view of the reported Fe deficiency-induced changes in protein amounts [11] and phosphorylation [13] we addressed the question whether and how Fe-deficiency affects the root 14-3-3 interactome, which is phosphorylation dependent. To this end, we carried out a semi-quantitative interactome analysis by affinity-purification mass spectrometry (qAP-MS) to assess Fe deficiency induced changes in 14-3-3/target interaction. To exclude proteins that bind non-specifically to the beads, we also performed a mock pull-down with empty beads along with the test pull-down experiments (Figure S2). In this experiment, we included the “unused” values generated from the software ProteinPilot [24]. After removal of

contaminant and false positive interactors (for details see M&M), a curated list of 117 14-3-3 interacting proteins was identified in the Wt roots (+ and -Fe), with unused value >2 in at least 2 independent samples remained (Table S1). These proteins are either so-called primary interactors (bind directly to 14-3-3) or secondary interactors (part of a multiprotein complex of which one protein is a primary interactor). We assigned the identified 14-3-3-interacting proteins to different functional categories, as shown in Figure 4. The majority of the identified proteins are related to carbohydrate and energy metabolism, metabolism, stress response, protein folding, cell structure and signaling. A comparison between our results (Table S1) and published 14-3-3 interactome studies shows that around 20% of the 14-3-3 interactors identified in this study have been previously reported as 14-3-3 interactors [7,17,25,26]. Sixteen proteins from our list were reported as Fe-responsive proteins, amongst which several enzymes involved in S-adenosylmethionine synthesis, two cytosolic invertases, Ferretin-1, the germin-like protein GLP5 (a plasmodesmata-localized proteins involved in the regulation of primary root growth) [27] and others [11,13,28]. As will be discussed later, the 14-3-3 interactome is not a random collection of proteins, but consists of distinct networks of interrelated proteins and protein complexes, involved in mitochondrial respiration, glycolysis, the methionine cycle, protein synthesis and folding and protein complexes of the head structure of the FoF1-synthase and vacuolar V-ATPase, tubulins and the TCP-1/cpn60/HSP chaperones (Table S2).

Comparison of 14-3-3 interactome under control and Fe deficient conditions. To study the dynamics of target interaction with 14-3-3 in response to Fe deficiency, we compared the abundance of identified proteins from Wt and *klun* roots grown under Fe sufficient and Fe deficient (for 24 h) condition, based on normalized intensity-based absolute quantification (iBAQ) values (normalized to the bait proteins in that run). The iBAQ intensities act as a measure of protein abundance and can be used to compare protein abundance between different samples. Among the 117 identified proteins, 27 and 18 proteins were significantly changed upon Fe deficiency in Wt and *klun*, respectively (Table 1& Figure 4). In Wt group, 12 proteins showed enhanced interaction and 14 proteins showed a reduction in interaction of which 5 were completely lost in the pull-down. These differential binding proteins are mainly involved in carbohydrate and energy metabolism, S-adenosylmethionine synthesis and stress response. In *klun* group, 7 proteins were increased and 10 proteins were decreased

in the pull-down. We found that most of the differential proteins identified in Wt and *klun* did not overlap. Among the significantly changed proteins identified from Wt and *klun*, 8 proteins in Wt showed similar trend as those in *klun* upon Fe deficiency, e.g. an adenosylmethionine synthase (SAM1) and an ATP synthase (ATP1). In addition, 15 proteins solely exhibited significantly different accumulation in Wt and 10 proteins in *klun* upon Fe deficiency. Particularly, 7 proteins including a neutral invertase (CINV2), PHOS32 and VIP3 were solely identified in Wt plants. Amongst the proteins that were lost in the 14-3-3 pull-down with protein extract form Wt plants, ECIP1 (EIN2 C-terminus interacting protein 1) may be relevant in view of the role of ethylene in Fe deficiency adaptation. ECIP1 is an MA3 domain-containing protein that interacts with EIN2, a central membrane protein that acts downstream of ethylene receptors, and upstream of ethylene regulated transcription factors. ECIP1 directly interacts with EIN2 and loss-of-function of ECIP1 resulted in enhanced ethylene response [29]. If ECIP1/14-3-3 interaction prevents ECIP1 breakdown as is e.g. the case for ABF3 [30], then loss of interaction between ECIP1 and 14-3-3 will result in enhanced ethylene signaling. So, this warrants further investigation.

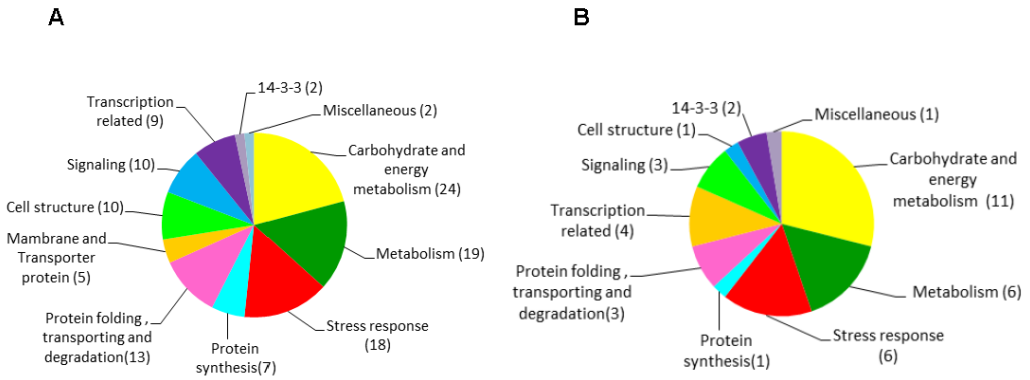

Figure 4. Grouping of identified target proteins according to functional categories. Pie chart of all 117 identified target proteins grouped according to functional categories (Table S1).

Moreover, a comparison of the *klun* interactome at sufficient Fe with that of Wt shows that over 90% of all identified interactors are present in both the Wt and *klun* pull-down. However, there are significant quantitative differences and a few proteins are even absent in the pull-down from either of the two genotypes (Table 2). The *klun* interactome lacks 7 proteins of the Wt interactome and vice versa the Wt interactome

lacks 4 proteins of the *klun* interactome. Moreover, 17 proteins are 3- to 4-fold enriched in the *klun* interactome as compared to Wt, whereas only 3 proteins are enriched in the Wt interactome as compared to *klun*. So, the absence of the four 14-3-3 isoforms in the *klun* mutant has a clear impact on the 14-3-3 interactome and it is noteworthy that many proteins are enriched in the *klun* interactome, what cannot be the result of a loss of *in vivo* phosphorylation in the absence of the four 14-3-3 proteins, as discussed above. It is difficult to predict how the absence of four 14-3-3 proteins, as is the case in the *klun* mutant, will affect the interactome. On the one hand, it may reduce *in vitro* interaction because *in vivo* binding of 14-3-3 proteins to a phosphorylated motif in target proteins enhances the *in vivo* level of phosphorylation as the site is then protected from dephosphorylation by phosphatases. On the other hand, the absence of 14-3-3s may result in more target protein in the pull-down because 14-3-3 can act as repressors of transcription factors or kinases. An example of the latter is the suppression of SOS2 activity by 14-3-3 binding [31]

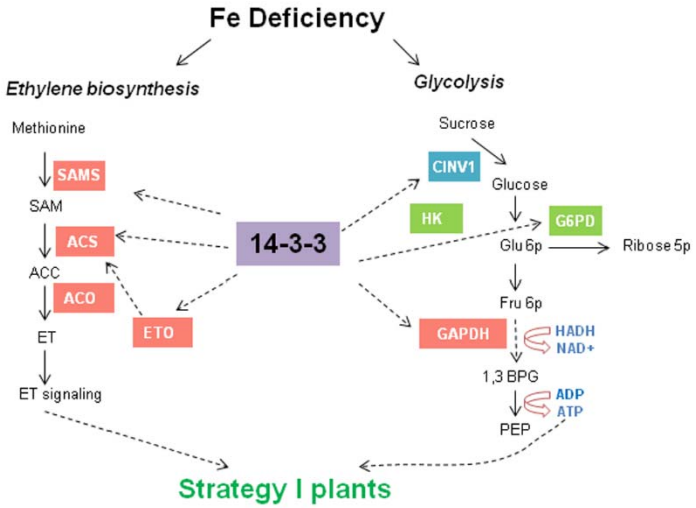

Figure 5. Model depicting the effect of Fe deficiency on 14-3-3 interacting proteins with a role in ethylene biosynthesis and glycolysis. Fe deficiency induces ethylene production by up-regulating SAMS, ACS and ACO genes (in red); Fe deficiency increases the activity of GAPDH (in red) and down-regulates the phosphorylation level of CINV1 (in blue) in glycolysis pathway. Green symbol indicates the relationship is not clear between Fe deficiency and G6PD and HK. 14-3-3 proteins regulate the activity of many enzymes in these pathways through direct or indirect interaction. SAMS, S-adenosyl metionine synthetase; ACS, ACC synthase; ACO, ACC oxidase; ETO, ethylene-overproducer; CINV1, alkaline invertase1; HK, hexokinase; GAPDH, glyceraldehyde-phosphate dehydrogenase; G6PD, Glucose-6-phosphate 1-dehydrogenase.

DISCUSSION

14-3-3 Proteins regulate the activities of a wide array of targets via direct protein–protein interactions and play a crucial role in many metabolic pathways [32]. Several studies have implied that 14-3-3 proteins have crucial roles in Fe deficiency [4,11,12]. In a detailed microarray analysis, a member of 14-3-3 epsilon group, GRF11 (14-3-3 Omicron) was significantly induced in the root elongation and maturation zone after subjecting plants to Fe deficiency for 24 h [33]. In addition, loss of function of GRF11 resulted in the failure of acidification and ferric chelate reductase (FCR) induction, and thus decreased Fe uptake. Moreover, expression of IRT1, FRO2, and AHA2, were repressed in the grf11 mutant both under Fe-deficient and under Fe-sufficient conditions [4]. However, another two 14-3-3 isoforms, GRF9 (14-3-3 Mu, Epsilon group member) and GRF1 (14-3-3 Chi, non-Epsilon group member) did not show a noticeable difference in expression in a Northern analyses in Arabidopsis under iron deficiency [16]. Previous quantitative proteomics [11,12] as well as a phosphoproteomics [13] studies towards Fe deficiency suggested that some 14-3-3 putative targets, such as Fructose-bisphosphate aldolase, Glucose-6-phosphate, cytosolic alkaline invertase 1 (CINV1), Nitrate reductase and H^+-ATPase were induced to change by Fe deficiency in Arabidopsis roots. Interestingly, transcripts of the protein elongation factor eIF5A, another putative 14-3-3 target, are also preferentially translated upon Fe deficiency, suggesting upstream regulatory factors [11]. In this study, we compared the physiological responses to Fe deficiency of Wt and three 14-3-3 quadruple mutant lines (*klpc*, *klun* and *unpc*), which were generated by crossing two double mutants: *kl*pc*, *kl*un* and *un*pc*. Next, we conducted a qAP-MS to analyze the 14-3-3 interactomes of roots in response to Fe deficiency (Wt, -Fe/+Fe) and in the *klun* mutant compared to Wt (Wt/*klun*, +Fe).

Fe deficiency is a major nutritional disorder that causes decreases in vegetative growth and marked yield and quality losses[34]. In this study, the 14-3-3 qKOs performed distinctly in response to long-term Fe deficiency at physiological levels. We found that *klpc* showed a significant growth reduction of both shoot and root at 2 μM Fe, whereat *unpc* showed the strongest growth reduction of shoot and root at 0 μM Fe (Figure S1). In addition, the Fe deficiency caused a much higher IUE (Iron Use Efficiency) of Wt shoot and root than that of the 14-3-3 mutants, what points to a more efficient use of available Fe in the Wt plants and thus to a role for 14-3-3 proteins in Fe-translocation

and/or use after uptake from the medium. The uptake of Fe by *klpc* and *klun* is clearly better than that of Wt, the use of Fe by Wt plants to sustain growth is better at the lowest medium Fe concentrations. A previous study has observed that the six 14-3-3 genes studied in this research have isoform specificity and redundancy in primary root growth and root cell elongation under various abiotic stresses [18]. According to our data, the mutant plants that combine *kl* with *un* (*klun*) or *kl* with *pc* (*klpc*) mutations showed a better Fe uptake than Wt plants at low medium Fe, while this phenotype was absent in *unpc* mutant. This indicated that the combination of kappa and lambda present isoform specificity amongst the 14-3-3 genes tested. Whether there is redundancy between the kappa and lambda requires further tested by analyzing the triple, double and single mutants.

H^+-ATPases (AHA2), FIT, FRO2 and IRT1 together mediate Fe deficiency induced medium acidification and Fe uptake in Strategy I plants. Fe deficiency induces FIT expression and FIT regulates the expression of AHA2, FRO2 and IRT [35-37]. Recently, 14-3-3 OMICRON (GRF11) was shown to act downstream of NO and further regulate FIT expression [4]. In this study, the expression of *14-3-3 OMICRON*, *FIT*, *FRO2* and *IRT1* were all induced by Fe deficiency, and their expression levels were significantly higher in the *klun* line than in Wt plants under Fe deficiency (Fig. 3). This suggests that somehow the KLUN proteins act as negative regulators of gene expression when the plants are Fe-starved. Moreover, in the *klpc* line the expression level of 14-3-3 OMICRON was not affected by Fe deficiency, accordingly FIT and FRO2 also failed to respond to Fe deficiency. Furthermore, a concurrent increase in the transcript levels of FIT and FRO2 with higher expression of 14-3-3 OMICRON in *klpc* under Fe-sufficient condition was also observed. Functional redundancy and isoform specificity associated with different mineral nutrients has been observed for 14-3-3 proteins. For example, P, K or Fe deprivation induced differential regulation of the genes encoding different isoforms of 14-3-3s in tomato roots [16,23]. So far, 14-3-3 OMICRON was the only 14-3-3 isoform reported to show different expression on Fe deficiency [4,33,36,38,39]. Van Kleeff et al. have demonstrated that phenotypic differences are consistent with isoform-specific functions and potential antagonistic functions between higher order Arabidopsis 14-3-3 mutants under abiotic stress conditions [18]. Although we observed that the 14-3-3 qKOs affected the expression of Fe deficiency induced genes, it remains

a question whether this regulation is affected directly by the mutations or indirectly by the 14-3-3 OMICRON taking over other's function (redundancy).

Recently, high-throughput "omics" analyses have been applied in iron deficiency studies and have provided a network of Fe deficiency adaptation mechanisms at the transcriptional, metabolic and protein level [11,13,40,41]. López-Millán *et al*. reviewed the common changes in the root proteome induced by Fe deficiency among different species [28], and stated that the increases in glycolysis and TCA cycle enzymes upon Fe deficiency were common amongst different species. For instance, fructose 1,6-bisphosphate aldolase and enolase were increased in three of the five plant species and catalase-2 was decreased in *P.persica* and *S. lycopersicum* upon Fe deficiency. In addition, Fe deficiency may cause changes in post-translational modifications as well. Several protein kinases (e.g. MPK3/MPK6) accumulatedifferentially upon Fe-deficient plants, what suggests that alterations in protein phosphorylation induced by Fe-deficiency are involved in Fe homeostasis[42]. A quantitative analysis of Fe deficiency-induced changes in the phospho-proteome profile of *Arabidopsis* roots showed that Fe deficiency induces changes in the phosphorylation of 45 proteins, with a suggested role in auxin homeostasis, RNA metabolism, carbohydrate flow, nitrate assimilation/amino acid synthesis and transport processes at the plasma membrane [13]. In this study, we applied quantitative affinity-purification mass spectrometry (qAP-MS) proteomics to analyze how the 14-3-3 interactome changes upon Fe deficiency. It must be noted that proteins found in the 14-3-3s affinity purification include not only primary or direct 14-3-3 targets but also secondary or indirect targets as members of multi protein complexes containing 14-3-3s. In total, almost 117 proteins were identified in our pull-down assays. Of these, a number have been identified and characterized as 14-3-3 binding targets in vivo or in vitro, such as EIF4A [43], FoF1-synthase[44], V-ATPase [45], CINV1 [46] and CPK3 [3]. Moreover, a comparison of our protein list with previous proteomics studies, revealed that 24 proteins have been identified in other 14-3-3s interactome studies, such as fructose-bisphosphate aldolase [17,26], MAT3 [17], TUA4/TUA2 [26], CINV1 [7,25], ATMS1 [7,26] and beta-fructofuranosidase invertase [7]. In addition, 8 of them were also reported as Fe-responsive proteins, including a fructose-bisphosphate aldolase, two cytosolic invertases, a 5-methyltetrahydropteroyltriglutamate-homocysteine methyltransferase, an S-adenosylmethionine synthase, a Germin-like protein and two Tubulins [11,28,47] (Table S1). An analysis of the interaction network of all identified

proteins using the STRING system (http://string.embl.de) shows that 46 of these can be assigned to protein complexes or functional networks (Table S2): mitochondrial FoF1-synthase, the vacuolar V-ATPase, elongation factors, chaperones, Cysteine/methionine synthesis and glycolysis/TCA cycle.

Since most proteins were found with high abundance in all pull-down experiments, it is difficult to directly assess the dynamic response of 14-3-3 interactions to Fe deficiency. Thus, quantitative analysis of the identified 14-3-3 clients is essential to reveal responses to Fe deficiency. Changes in 14-3-3 interaction may be due to changes in protein abundance and protein phosphorylation: events that were shown to be crucial for the Fe deficiency response [11,13]. Thus, changes of interaction with 14-3-3s can have two causes: 1) Fe deficiency regulates the expression of 14-3-3 targets, like that of FIT [4] and fructose-bisphosphate aldolase [11] and 2) the phosphorylation level of 14-3-3 binding targets is different under Fe-deficient conditions, as reported for CINV1, AHA1 and MAPKKK [13].

By comparing the normalized iBAQ, we found that 28 and 18 proteins were significantly changed in the 14-3-3 interactome of Wt and *klun* upon Fe deficiency treatment, respectively (Table 1). Moreover, a comparison of the Wt and *klun* interactome of Fe sufficient roots showed a quantitative or absolute difference in the interaction of 32 proteins (Table 2). So, the 14-3-3 interactome is clearly affected by Fe deficiency (Wt, -/+Fe) as well as by the absence of four 14-3-3 isoforms (Wt/*klun*, +Fe). The observed changes are mainly in proteins with a function in carbohydrate and energy metabolism and cysteine/methionine synthesis and we will therefore limit our discussion to these pathways. An increase in $NADH^+$ ATP production by activation of the glycolytic pathway and mitochondrial respiration can provide the reducing equivalents to keep the Fe (III) reductase working and fuel the plasma membrane ATPase: processes that are essential for the Fe-uptake mechanism in iron-deficient roots [48]. Cysteine/methionine synthesis is important in the Fe deficiency response as it provides the precursors for ethylene and nicotianamine (NA), an important chelator with a crucial function role in Fe homeostasis and transport [49].

14-3-3 proteins are involved in carbon and nitrogen metabolism by interacting with nitrate reductase (NR) and sucrose phosphate synthase (SPS), which are the more extensively characterized 14-3-3 target proteins [50]. In this study, changes of protein

abundance in carbohydrate and energy metabolism enzymes upon Fe deficiency are consistently identified among different proteomics studies [28]. Moreover, alterations in protein phosphorylation patterns induced by Fe deficiency are likely to be associated with primary carbohydrate metabolism [13]. Increases in the activities and concentrations of enzymes such as fructose 1,6-bisphosphate aldolase, enolase, triosephosphate isomerase and GAPDH have been observed in Fe-deficient root extracts in many studies [28,51,52]. Our results show that enzymes involved in sugar metabolism, glycolysis and TCA cycle are 14-3-3 targets (Table S2). The interactions with these proteins in Wt were responsive to Fe deficiency (Table 1): both increased interaction (FBA8, GAPCP-1) and decreased interaction (G6PD3, CINV2) was observed. The *klun* mutant showed higher levels of interaction of GAPC1 and GAPC2 and a loss of CINV2 interaction at Fe sufficient condition as compared to Wt (Table 2). These results warrant a functional analysis of how 14-3-3 affects the activity of the glycolytic/TCA enzymes, as nothing is known about that so far. In our previous study, the CINV1 activity was shown to be positively regulated by 14-3-3 proteins [46]. Here, CINV1 did not show different binding to 14-3-3s in Wt (-Fe/+Fe), but the amount of interacting CINV1 was two-fold higher in *klun* as compared to Wt (Table 2). The closely related CINV2 protein was found to be reduced in the Wt upon Fe deficiency. It is also noteworthy that other sugar and glycolysis related enzymes known to interact with 14-3-3s, like SPS, TPS1 and F2KP [46,53-55] were not found in our study.

Fe acquisition mechanisms demand reducing power and energy in the form of NADH and ATP [28] and increased mitochondrial respiration is a classical response to Fe deficiency to fuel the plasma membrane ATPases [56]. We identified three subunits of the mitochondrial ATP synthase head structure (α, β and δ), NADH dehydrogenase and the mitochondrial-processing peptidase MPPBETA. FoF1-synthase has been reported as 14-3-3 target [44,45] and the identification of only subunits of the head-structure is in line with the evidence that the β-subunit is the direct target for 14-3-3. Functionally, the mitochondrial synthase activity is reduced by interaction with 14-3-3 [44] and in that respect it is surprising that in Wt, Fe deficiency enhances the interaction with the FoF1-subunits and the mitochondrial processing peptidase 2- to 10-fold (Table 2). This increased interaction suggests a down-regulation of the ATP-synthase, what is contrary to the expected increase in respiration. Interaction with MPPBETA and CI51 is increased 3- to 10-fold respectively and this warrant further study of the functional

consequences of 14-3-3/MPPBETA and CI51 interaction. It should be noted that the related head structure of the vacuolar V-ATPase (A, B and E1 subunits) was isolated as well, but Fe deficiency had no effect on the interaction with the V-ATPase.

Enhanced ethylene production is a well described response to Fe deficiency [57]. Fe deficiency induced multiple S-adenosylmethionine synthases (gene expression and protein amount) involved in S-adenosyl-Met [58] biosynthesis, an important precursor for ethylene production [11]. 14-3-3s are linked to the ethylene biosynthesis by interacting with S-adenosylmethionine synthase [58], ACC synthase and 1-aminocyclopropane-1-carboxylate synthase (ACS) [17,25,59,60]. Here, we identified four S-adenosylmethionine synthases (SAM1, SAM2, SAM3, and MTO3) and the 5-methyltetrahydropteroyltriglutamate-homocysteine methyltransferase (ATMS1) in the 14-3-3s interactome, underlining the importance of 14-3-3s in this pathway (Table S1 and S2). Fe-deficiency stimulated the interaction with SAM1, but reduced the interaction with MTO3 and ATMS1 in Wt (Table 1). The interaction of these proteins in *klun* at sufficient Fe was comparable to that of Wt. SAM is not only a precursor for ethylene biosynthesis, but also for the production of nicotianamine (NA), a chelator important for Fe homeostasis [61]. Figure 5 shows a model incorporating the role of 14-3-3 in ethylene biosynthesis and glycolysis in relation to Fe deficiency adaptation. It is difficult to draw further conclusions as to the consequences of the differential responses of the SAM-synthases to Fe deficiency: clearly the SAM-synthase/14-3-3 interaction is important in the Fe adaptation response and it is of prime importance to address the question how 14-3-3s affect the SAM-synthase activities.

MATERIALS AND METHODS

Plant growth conditions. All plants used are in the *Arabidopsis thaliana* Columbia ecotype (Col-0) background. The 14-3-3 quadruple KO mutants were generated by crossing the double mutants as described in the previous study reported by van Kleeff et al [18]. The mutant seeds collection and plants growth were carried out with the permission from the Vrije University Amsterdam. Experimental research using plants comply with institutional, national, or international guidelines.

Plants were grown in ½ strength Hoagland solution (pH 5.8) with 20 µM Fe(III)-EDTA in a growth chamber at 14/10h day/night regime, 22/18 °C day/night temperature and a photon flux density of 170 µmol•m-2•s-1. After 22 days of germination, plant roots were washed with once with 1 mM EDTA followed by two times wash in Milli Q, before transfer to either iron-sufficient (20 µM Fe(III)-EDTA) or iron-deficient (iron omitted) culture medium for 24 hours. Then the roots were harvested and immediately cleaned with Milli Q. After that, the roots were dried on tissue paper and snap frozen in liquid nitrogen. Total roots were ground in liquid nitrogen and weighed, and stored at -80°C. The plant material was used for 14-3-3 pull-down experiments. For growth and Fe content measurement, plants of Wt and 14-3-3 qKO plants were grown in ½ strength Hoagland solution (pH 5.8) with 20 µM Fe(III)-EDTA for 14 days, then young seedlings were transplanted to a new medium supplemented with 0, 2, 5, and 20 µM Fe(III)-EDTA. Leaves and roots were harvested 12 days after Fe deficient treatment. Before harvest, the roots were washed as described above. The collected shoots and roots from two plants were pooled for each biological replicate and harvested separately and dried at 150 °C for 2 days.

Analysis of the Fe content in Arabidopsis shoots and roots. Fe content in Arabidopsis leaves and roots was determined by the BPDS (bathophenanthroline disulfonic acid) method as described previously by Schmidt [62]. In brief, 4 to 8 mg dried sample was well mixed in 2 mL Eppendorf tubes and heated at 95 °C in 75 µL nitric acid (65%) for 6 h. After the samples were completely digested, 50 µL of H_2O_2 (30%) was added, and the solution was incubated at 56 °C for 2 h. The volume was adjusted to 200 µL with sterile water. 20 µL of this solution was diluted in 980 µL of BPDS buffer (1 mM BPDS, 0.6 M sodium acetate, and 0.48 M hydroxylammonium chloride). The concentration of Fe-BPDS was measured at 535 nm. A standard curve was prepared by dilution of a stock $FeSO_4$ solution dissolved in 0.1 M HCl.

Real-time PCR assay. Total RNA was extracted from root tissues using the NucleoSpin® RNA Plant Kit (MACHEREY-NAGEL), and first-strand cDNA was synthesized from 2 µg of total RNA using the Superscript II Kit (Invitrogen, USA) with oligo d(T)18 primers according to the manufacturer's instructions. Quantitative RT-PCR reaction contained 100 ng cDNA, 1 pmol of each primer, 2x Sybr Green PCR buffer (Bio-Rad, Hercules). The PCR conditions for the amplification of *14-3-3 omicron*, *FIT*, *FRO2*, *IRT1*, *AHA2* and *ubiquitin 10* were as follows: 1 min at 94 °C, followed by 30 cycles of 45 s at 94 °C, 60 s at 54 °C and 75 s at 72 °C. The PCR products were examined according the 2-ΔΔCT method. Each sample was assayed three times. The relative expression was calculated against that of the internal control gene ubiquitin 10 (UBQ10). Primer pairs used for each gene are listed in Table S3.

Affinity purification of 14-3-3 target proteins. Recombinant His-tagged proteins were purified as described in [46]. Protein concentrations were determined by Bradford micro-assay (Bio-Rad) using BSA as a standard. Arabidopsis roots from WT and *klun* plants were ground in liquid nitrogen and extracted with extraction buffer (50 mM HEPES-NaOH (pH 7), 10 mM $MgCl_2$, 1 mM Na_2EDTA, 2 mM DTT, 10% ethylene glycol, 0.02% Triton, 1× protease inhibitor cocktail and 1× phosSTOP). Protein extracts were centrifuged twice at 20,000g for 15 min. To avoid the isoform specifically binding of the 14-3-3 target proteins, equal amount of four 14-3-3 isoforms (His-KAPPA, His-LAMBDA, His-NU, His-UPSILON) were well mixed and then coated to PureProteome™ Nickel magnetic Beads (Millipore) according to manufactures' protocol. Protein extracts were collected from roots of *klun* and WT treated with 0 and 20 µM Fe(III)-EDTA for 24 hours. After coating of 40 µg of His-14-3-3 to 100 µl nickel beads and extensive washing with binding buffer (50 mM sodium phosphate, 300 mM sodium chloride, 10 mM imidazole, pH 8), 2 mg protein extract was added to the 14-3-3 beads and incubated overnight at 4 ºC. To distinguish background proteins, we performed mock pull-down with empty beads, where the extracts were incubated with beads that were not coated with His-14-3-3. Beads were extensively washed in 1 ml wash buffer containing 10 mM imidazole for 5 min and this was repeated 5 times. The bound protein complexes were eluted off from beads with 100 µl of wash buffer containing 100 mM imidazole for 20 min. The experiment was conducted three times

with independent biological replicates, meaning that in the end each genotype had 6 profiles. CBB-stained gel was used as the loading control (Figure S2). The affinity-enriched proteins were separated on SDS-PAGE, and then characterized by LC-MS-MS semi-quantitatively.

In-gel digestion and LC-MS/MS analysis. LC-MS/MS Analysis and Comparative Proteomic Analysis Proteins from pull-down experiments were resolved on a one-dimensional 10% SDS polyacrylamide gel. After staining with Coomassie Blue, each sample lane was divided into four pieces. Each gel slice was cut into small particles and transferred to a clean micro-centrifuge tube. For in-gel digestion, 50 % acetonitrile containing 50 mM $(NH_4)HCO_3$ was added and vortexed until the Coomassie brilliant blue was completely removed. To reduce the cysteine residues, each gel band was covered with a 10 mM DTT solution prepared in 50 mM $(NH_4)HCO_3$ for 60 min at 56 °C. The DTT solution was removed, and the excised bands were incubated with 55 mM iodoacetamide prepared in 50 mM $(NH_4)HCO_3$ for 40 min in the dark. The iodoacetamide solution was then removed. After washing the gel particles three times with 50 mM $(NH_4)HCO_3$ for 10 min, dehydration was performed with 100% acetonitrile for 10 min. The gel particles were then vacuum-dried for 20 min and rehydrated with 12.5 μg/μL trypsin (Promega) in 50 mM $(NH_4)HCO_3$ buffer. Digestion was performed by incubation at 37 °C overnight. Following digestion, tryptic peptides were extracted with 100 μl of 50 % acetonitrile/1 % acetic acid for 20 min. The tryptic peptides were dried with speed-vac, re-dissolved in 40 μl 0.1% acetic acid and subjected to LC-MS/MS analysis as described by Chen et al (Chen, van der Schors et al. 2011). In short, 20 μL peptides were loaded on a 5 mm Pepmap 100 C18 (Dionex) column (300 μm ID, 5μm particle size) and separated on a 200 mm Alltima C18 homemade column (100 μm ID, 3μm particle size) with an Eksigent HPLC system, using a linear gradient of increasing acetonitrile concentration from 5% to 35% in 45 min, and to 90% in 5 min. The flow rate was 400 nL/min. The eluted peptides were electro-sprayed into the LTQ-Orbitrap discovery. The mass spectrometer was operated in a data dependent

manner with one MS (m/z range from 330 to 2000) followed by MS-MS on five most abundant ions. The exclusion window was 25 sec. MS/MS spectra were searched against an IPI Arabidopsis database (ipi.ARATH.v3.85) with the ProteinPilot™ software (version 3.0; Applied Biosystems, Foster City, CA, USA; MDS Sciex) using the Paragon algorithm (version 3.0.0.0) as the search engine. The search parameters were set to cysteine alkylation with acrylamide, and digestion with trypsin. Detected protein threshold was set in protein summary to 0.5 achieving a 20% confidence. In this experiment, we included the unused values generated from the software ProteinPilot[24]. The 'unused' value is defined as a summation of protein scores from all the non-redundant peptides matched to a single protein. Peptides with confidence of >99% have a protein score of 2; >95% have a protein score of 1.3, >66% have a protein score of 0.47, etc. The mass spectrometric data was searched against the Uniprot proteomics database (version 2013-01-06) with the Max-Quant software (version 1.3.0.5) to obtain peptides and proteins identified in each experiment. The search parameters were: MS accuracy 6 ppm, MS-MS accuracy 0.5 Da, fixed modification of cysteine alkyation with acrylamide, variable modification of methionine oxidation and protein N-terminal acetylation, digestion with trypsin, protein hits containing at least one unique peptide, and false discovery rates of both peptides and proteins within 0.01.

Data analysis. To increase the data quality, we removed the low confident interacting proteins from the protein list. First, contaminant proteins like keratin and trypsin were removed from this results file. Second, considering the reproducibility of the pull-down experiment, we excluded proteins that were identified only once in all replicates. False positives were removed from the bait-prey matrix by comparing the abundance of proteins identified in each pull-down against their abundance in the matching empty bead controls, in which the true positive bait-prey interactions should be >10-fold enriched in the APs. Also, the four bait proteins were excluded from the list.

Intensity-based absolute quantification (iBAQ) values were calculated in the Max-Quant suite as previously described [63,64]. The protein abundance was calculated on the basis of the normalized iBAQ intensity. For short, quantifiable proteins in the analysis defined as those identified in at least two of the three biological replicates in at least

one type of sample. Missing values were imputed using row mean imputation. The relative protein intensities were calculated as the ratio of their intensity to the bait proteins in that run. The relative protein intensities for each pull-down experiment were combined in a matrix, and false positives were removed the proteins identified in the background. The minimum two requirements for the differentially expressed proteins are: (i) identification of a protein with unused value >2; (ii) the fold change of protein quantities protein quantities in Fe-deficient treated samples against Fe-sufficient samples with more or less than 1.5 times with significant difference Student's t-test P-value <0.05).

Reference

1 Vert, G. A., Briat, J. F. & Curie, C. Dual regulation of the Arabidopsis high-affinity root iron uptake system by local and long-distance signals. *Plant Physiology* **132**, 796-804, doi:10.1104/pp.102.016089 (2003).

2 Vert, G. *et al.* IRT1, an Arabidopsis transporter essential for iron uptake from the soil and for plant growth. *Plant Cell* **14**, 1223-1233, doi:10.1105/tpc.001388 (2002).

3 Lachaud, C. *et al.* 14-3-3-Regulated Ca2+-dependent protein kinase CPK3 is required for sphingolipid-induced cell death in Arabidopsis. *Cell Death and Differentiation* **20**, 209-217, doi:10.1038/cdd.2012.114 (2013).

4 Yang, J. L. *et al.* The 14-3-3 protein GENERAL REGULATORY FACTOR11 (GRF11) acts downstream of nitric oxide to regulate iron acquisition in Arabidopsis thaliana. *New Phytologist* **197**, 815-824, doi:10.1111/nph.12057 (2013).

5 Singh, S., Kailasam, S., Lo, J.-C. & Yeh, K.-C. Histone H3 lysine4 trimethylation-regulated GRF11 expression is essential for the iron-deficiency response in Arabidopsis thaliana. *New Phytologist* **230**, 244-+, doi:10.1111/nph.17130 (2021).

6 Gutierrez-Carbonell, E. *et al.* A Shotgun Proteomic Approach Reveals That Fe Deficiency Causes Marked Changes in the Protein Profiles of Plasma Membrane and Detergent-Resistant Microdomain Preparations from Beta vulgaris Roots. *Journal of Proteome Research* **15**, 2510-2524, doi:10.1021/acs.jproteome.6b00026 (2016).

7 Swatek, K. N., Graham, K., Agrawal, G. K. & Thelen, J. J. The 14-3-3 Isoforms Chi and Epsilon Differentially Bind Client Proteins from Developing

Arabidopsis Seed. *Journal of Proteome Research* **10**, 4076-4087, doi:10.1021/pr200263m (2011).

8 Cardasis, H. L. *et al.* FTICR-MS analysis of 14-3-3 isoform substrate selection. *Biochimica Et Biophysica Acta-Proteins and Proteomics* **1774**, 866-873, doi:10.1016/j.bbapap.2007.05.004 (2007).

9 Bornke, F. The variable C-terminus of 14-3-3 proteins mediates isoform-specific interaction with sucrose-phosphate synthase in the yeast two-hybrid system. *Journal of Plant Physiology* **162**, 161-168, doi:10.1016/j.jplph.2004.09.006 (2005).

10 Pallucca, R. *et al.* Specificity of epsilon and Non-epsilon Isoforms of Arabidopsis 14-3-3 Proteins Towards the H+-ATPase and Other Targets. *Plos One* **9**, doi:10.1371/journal.pone.0090764 (2014).

11 Lan, P. *et al.* iTRAQ Protein Profile Analysis of Arabidopsis Roots Reveals New Aspects Critical for Iron Homeostasis. *Plant Physiology* **155**, 821-834, doi:10.1104/pp.110.169508 (2011).

12 Rodriguez-Celma, J. *et al.* Root Responses of Medicago truncatula Plants Grown in Two Different Iron Deficiency Conditions: Changes in Root Protein Profile and Riboflavin Biosynthesis. *Journal of Proteome Research* **10**, 2590-2601, doi:10.1021/pr2000623 (2011).

13 Lan, P., Li, W., Wen, T.-N. & Schmidt, W. Quantitative Phosphoproteome Profiling of Iron-Deficient Arabidopsis Roots. *Plant Physiology* **159**, 403-417, doi:10.1104/pp.112.193987 (2012).

14 Roberts, M. R. & de Bruxelles, G. L. Plant 14-3-3 protein families: evidence for isoform-specific functions? *Biochemical Society Transactions* **30**, 373-378 (2002).

15 Paul, A. L., Denison, F. C., Schultz, E. R., Zupanska, A. K. & Ferl, R. J. 14-3-3 Phosphoprotein interaction networks - does isoform diversity present functional interaction specification? *Frontiers in Plant Science* **3**, doi:10.3389/fpls.2012.00190 (2012).

16 Cao, A., Jain, A., Baldwin, J. C. & Raghothama, K. G. Phosphate differentially regulates 14-3-3 family members and GRF9 plays a role in Pi-starvation induced responses. *Planta* **226**, 1219-1230, doi:10.1007/s00425-007-0569-0 (2007).

17 Shin, R., Jez, J. M., Basra, A., Zhang, B. & Schachtman, D. P. 14-3-3 Proteins fine-tune plant nutrient metabolism. *Febs Letters* **585**, 143-147, doi:10.1016/j.febslet.2010.11.025 (2011).

18 van Kleeff, P. J. *et al.* Higher order Arabidopsis 14-3-3 mutants show 14-3-3 involvement in primary root growth both under control and abiotic stress conditions. *J Exp Bot* **65**, 5877-5888 (2014).

19 Jaspert, N., Throm, C. & Oecking, C. Arabidopsis 14-3-3 proteins: fascinating and less fascinating aspects. *Frontiers in Plant Science* **2**, doi:10.3389/fpls.2011.00096 (2011).

20 Vanheusden, G. P. H. *et al.* THE 14-3-3-PROTEINS ENCODED BY THE BMH1 AND BMH2 GENES ARE ESSENTIAL IN THE YEAST SACCHAROMYCES-CEREVISIAE AND CAN BE REPLACED BY A PLANT HOMOLOG. *European Journal of Biochemistry* **229**, 45-53 (1995).

21 Brumbarova, T., Bauer, P. & Ivanov, R. Molecular mechanisms governing Arabidopsis iron uptake. *Trends in Plant Science* **20**, 124-133, doi:10.1016/j.tplants.2014.11.004 (2015).

22 Tissot, N. *et al.* Iron around the clock. *Plant Science* **224**, 112-119, doi:10.1016/j.plantsci.2014.03.015 (2014).

23 Xu, W. F. & Shi, W. M. Expression profiling of the 14-3-3 gene family in response to salt stress and potassium and iron deficiencies in young tomato (Solanum lycopersicum) roots: Analysis by real-time RT-PCR. *Annals of Botany* **98**, 965-974, doi:10.1093/aob/mcl189 (2006).

24 Klemmer, P., Smit, A. B. & Li, K. W. Proteomics analyses of immuno-precipitated synaptic protein complexes. *Journal of Proteomics* **72**, 82-90, doi:10.1016/j.jprot.2008.10.005 (2009).

25 Chang, I. F. *et al.* Proteomic profiling of tandem affinity purified 14-3-3 protein complexes in Arabidopsis thaliana. *Proteomics* **9**, 2967-2985, doi:10.1002/pmic.200800445 (2009).

26 Paul, A.-L. *et al.* Comparative Interactomics: Analysis of Arabidopsis 14-3-3 Complexes Reveals Highly Conserved 14-3-3 Interactions between Humans and Plants. *Journal of Proteome Research* **8**, 1913-1924, doi:10.1021/pr8008644 (2009).

27 Lindberg, J., Smith, R. & Peethambaran, B. Effects of 14-3-3 lambda on the biosynthesis of flavonoids in Arabidopsis thaliana. *Planta Medica* **78**, 1113-1113 (2012).

28 Lopez-Millan, A.-F., Grusak, M. A., Abadia, A. & Abadia, J. Iron deficiency in plants: an insight from proteomic approaches. *Frontiers in plant science* **4**, 254-254, doi:10.3389/fpls.2013.00254 (2013).

29 Lei, G. *et al.* EIN2 regulates salt stress response and interacts with a MA3 domain-containing protein ECIP1 in Arabidopsis. *Plant Cell and Environment* **34**, 1678-1692, doi:10.1111/j.1365-3040.2011.02363.x (2011).

30 Sirichandra, C. *et al.* The Arabidopsis ABA-Activated Kinase OST1 Phosphorylates the bZIP Transcription Factor ABF3 and Creates a 14-3-3 Binding Site Involved in Its Turnover. *Plos One* **5**, doi:10.1371/journal.pone.0013935 (2010).

31 Zhou, H. *et al.* Inhibition of the Arabidopsis Salt Overly Sensitive Pathway by 14-3-3 Proteins. *Plant Cell* **26**, 1166-1182, doi:10.1105/tpc.113.117069 (2014).

32 DeLille, J. M., Sehnke, P. C. & Ferl, R. J. The arabidopsis 14-3-3 family of signaling regulators. *Plant Physiology* **126**, 35-38, doi:10.1104/pp.126.1.35 (2001).

33 Dinneny, J. R. *et al.* Cell identity mediates the response of Arabidopsis roots to abiotic stress. *Science* **320**, 942-945, doi:10.1126/science.1153795 (2008).

34 Abadia, J., Lopez-Millan, A. F., Rombola, A. & Abadia, A. Organic acids and Fe deficiency: a review. *Plant and Soil* **241**, 75-86, doi:10.1023/a:1016093317898 (2002).

35 Jakoby, M., Wang, H. Y., Reidt, W., Weisshaar, B. & Bauer, P. FRU (BHLH029) is required for induction of iron mobilization genes in Arabidopsis thaliana. *Febs Letters* **577**, 528-534, doi:10.1016/j.febslet.2004.10.062 (2004).

36 Colangelo, E. P. & Guerinot, M. L. The essential basic helix-loop-helix protein FIT1 is required for the iron deficiency response. *Plant Cell* **16**, 3400-3412, doi:10.1105/tpc.104.024315 (2004).

37 Sivitz, A. B., Hermand, V., Curie, C. & Vert, G. Arabidopsis bHLH100 and bHLH101 Control Iron Homeostasis via a FIT-Independent Pathway. *Plos One* **7**, doi:10.1371/journal.pone.0044843 (2012).

38 Zamboni, A. *et al.* Genome-wide microarray analysis of tomato roots showed defined responses to iron deficiency. *Bmc Genomics* **13**, doi:10.1186/1471-2164-13-101 (2012).

39 Buckhout, T. J., Yang, T. J. W. & Schmidt, W. Early iron-deficiency-induced transcriptional changes in Arabidopsis roots as revealed by microarray analyses. *Bmc Genomics* **10**, doi:10.1186/1471-2164-10-147 (2009).

40 Lopez-Millan, A. F., Morales, F., Gogorcena, Y., Abadia, A. & Abadia, J. Metabolic responses in iron deficient tomato plants. *Journal of Plant Physiology* **166**, 375-384, doi:10.1016/j.jplph.2008.06.011 (2009).

41 Li, J., Wu, X.-D., Hao, S.-T., Wang, X.-J. & Ling, H.-Q. Proteomic response to iron deficiency in tomato root. *Proteomics* **8**, 2299-2311, doi:10.1002/pmic.200700942 (2008).

42 Ye, L. X. *et al.* MPK3/MPK6 are involved in iron deficiency-induced ethylene production in Arabidopsis. *Frontiers in Plant Science* **6**, doi:10.3389/fpls.2015.00953 (2015).

43 Freire ER *et al.* eIF4F-like complexes formed by cap-binding homolog TbEIF4E5 with TbEIF4G1 or TbEIF4G2 are implicated in post-transcriptional regulation in Trypanosoma brucei. *RNA* **20**, 1272-1286 (2014).

44 Bunney, T. D., van Walraven, H. S. & de Boer, A. H. 14-3-3 protein is a regulator of the mitochondrial and chloroplast ATP synthase. *Proceedings of the National Academy of Sciences of the United States of America* **98**, 4249-4254, doi:10.1073/pnas.061437498 (2001).

45 Klychnikov, O. I., Li, K. W., Lill, H. & de Boer, A. H. The V-ATPase from etiolated barley (Hordeum vulgare L.) shoots is activated by blue light and interacts with 14-3-3 proteins. *Journal of Experimental Botany* **58**, 1013-1023, doi:10.1093/jxb/erl261 (2007).

46 Gao J *et al.* Light modulated activity of root alkaline/neutral invertase involves the interaction with 14-3-3 proteins. *Plant Journal* **80**, 785-796 (2014).

47 Lan, P., Li, W. & Schmidt, W. A digital compendium of genes mediating the reversible phosphorylation of proteins in fe-deficient Arabidopsis roots. *Frontiers in plant science* **4**, 173-173, doi:10.3389/fpls.2013.00173 (2013).

48 Sijmons, P. C., Briel, W. v. d. & Bienfait, H. F. Cytosolic NADPH Is the Electron Donor for Extracellular FeIII Reduction in Iron-Deficient Bean Roots. *Plant Physiology* **75**, 219-221 (1984).

49 Klatte, M. *et al.* The Analysis of Arabidopsis Nicotianamine Synthase Mutants Reveals Functions for Nicotianamine in Seed Iron Loading and Iron Deficiency Responses. *Plant Physiology* **150**, 257-271, doi:10.1104/pp.109.136374 (2009).

50 Comparot, S., Lingiah, G. & Martin, T. Function and specificity of 14-3-3 proteins in the regulation of carbohydrate and nitrogen metabolism. *Journal of Experimental Botany* **54**, 595-604, doi:10.1093/jxb/erg057 (2003).

51 Rellan-Alvarez, R. *et al.* Changes in the proteomic and metabolic profiles of Beta vulgaris root tips in response to iron deficiency and resupply. *Bmc Plant Biology* **10**, doi:10.1186/1471-2229-10-120 (2010).

52 Brumbarova, T., Matros, A., Mock, H.-P. & Bauer, P. A proteomic study showing differential regulation of stress, redox regulation and peroxidase proteins by iron supply and the transcription factor FER. *Plant Journal* **54**, 321-334, doi:10.1111/j.1365-313X.2008.03421.x (2008).

53 Zuk, M., Weber, R. & Szopa, J. 14-3-3 Protein down-regulates key enzyme activities of nitrate and carbohydrate metabolism in potato plants. *Journal of*

Agricultural and Food Chemistry **53**, 3454-3460, doi:10.1021/jf0485584 (2005).

54 Kulma, A. *et al.* Phosphorylation and 14-3-3 binding of Arabidopsis 6-phosphofructo-2-kinase/fructose-2,6-bisphosphatase. *Plant Journal* **37**, 654-667, doi:10.1111/j.1365-313X.2003.01992.x (2004).

55 Bustos, D. M. & Iglesias, A. A. Phosphorylated non-phosphorylating glyceraldehyde-3-phosphate dehydrogenase from heterotrophic cells of wheat interacts with 14-3-3 proteins. *Plant Physiology* **133**, 2081-2088, doi:10.1104/pp.103.030981 (2003).

56 Espen, L., Dell'Orto, M., De Nisi, P. & Zocchi, G. Metabolic responses in cucumber (Cucumis sativus L.) roots under Fe-deficiency: a P-31-nuclear magnetic resonance in-vivo study. *Planta* **210**, 985-992, doi:10.1007/s004250050707 (2000).

57 Garcia, M. J., Suarez, V., Romera, F. J., Alcantara, E. & Perez-Vicente, R. A new model involving ethylene, nitric oxide and Fe to explain the regulation of Fe-acquisition genes in Strategy I plants. *Plant Physiology and Biochemistry* **49**, 537-544, doi:10.1016/j.plaphy.2011.01.019 (2011).

58 Phanchaisri, B., Samsang, N., Yu, L., Singkarat, S. & Anuntalabhochai, S. Expression of OsSPY and 14-3-3 genes involved in plant height variations of ion-beam-induced KDML 105 rice mutants. *Mutation Research-Fundamental and Molecular Mechanisms of Mutagenesis* **734**, 56-61, doi:10.1016/j.mrfmmm.2012.03.002 (2012).

59 Catalá, R. *et al.* The Arabidopsis 14-3-3 protein RARE COLD INDUCIBLE 1A links low-temperature response and ethylene biosynthesis to regulate freezing tolerance and cold acclimation. *Plant Cell* **26**, 3326-3342 (2014).

60 Yoon, G. M. & Kieber, J. J. 14-3-3 regulates 1-aminocyclopropane-1-carboxylate synthase protein turnover in Arabidopsis. *Plant Cell* **25**, 1016-1028 (2013).

61 Brumbarova, T. & Bauer, P. Iron-mediated control of the basic helix-loop-helix protein FER, a regulator of iron uptake in tomato. *Plant Physiology* **137**, 1018-1026, doi:10.1104/pp.104.054270 (2005).

62 Schmidt, W., Boomgaarden, B. & Ahrens, V. Reduction of root iron in Plantago lanceolata during recovery from Fe deficiency. *Physiologia Plantarum* **98**, 587-593 (1996).

63 Xu, W. *et al.* PIN2 is required for the adaptation of Arabidopsis roots to alkaline stress by modulating proton secretion. *Journal of Experimental Botany* **63**, 6105-6114, doi:10.1093/jxb/ers259 (2012).

64 Jagtap P *et al.* Workflow for analysis of high mass accuracy salivary data set using MaxQuant and ProteinPilot search algorithm. *Proteomics* **12**, 1726-1730 (2012).

Acknowledgments

We thank Ning Chen (Department of Molecular and Cellular Neurobiology, Faculty of Earth and Life Sciences, Vrije Universiteit Amsterdam) for her technical assistance with the project. The project was supported by a grant from the Netherlands Organization for Scientific Research (NWO; 817.02.006) to A.H. de Boer, and a grant from National Natural Science Foundation of China (No. 31802146) to Jing Gao.

Author Contributions

A.H. de Boer conceived and designed the experiments; Jing Gao performed the experiments; Paula J. M. van Kleeff generated the 14-3-3 mutant plants, Ka Wan Li contributed to analysis tools of proteomics data; Jing Gao wrote the manuscript with suggestions by A.H. de Boer, Paula J. M. van Kleeff. All authors have read and approved the final manuscript.

Competing Interests: The authors declare no competing interests.

Figure legends

Figure 1. Growth performance of Wt and 14-3-3 qKOs under different Fe deficiency treatment. After two weeks of growth on ½ strength Hoagland solution, plants were grown for an additional 12 days at 0, 2, 5 and 20 μM (= sufficient) Fe. Fresh weight of roots (A), shoots (B) were measured from Wt and 14-3-3 qKOs plants. Each bar represents the mean of 10 biological replicates. The line above each bar is the SE. Means with different superscripts are significantly different at $P<0.05$, by two-way ANOVA followed by Bonferroni's post hoc test.

Figure 2. Fe content of shoots and roots of WT and 14-3-3 qKOs plants. After two weeks of growth on ½ strength Hoagland solution, plants were grown for an additional 12 days at 0, 2, 5 and 20 μM (= sufficient) Fe. Shoots and roots were harvested, weighed and pooled per two for the Fe-determination. A and B, Fe-content of roots and shoots; C and D, Iron Use Efficiency (IUE) of roots and shoots. Each bar represents a mean of observations in 5 biological replicates, ± SE. Averages with different superscripts are significantly different at $P<0.05$, by two-way ANOVA followed by Bonferroni's post hoc test.

Figure 3. Expression analysis of 14-3-3 Omicron, FIT, FRO, IRT and AHA2 in Wt and 14-3-3 qKO lines grown with (plus) and without (minus) Fe. A. thaliana seedlings were grown in +Fe medium for 22 days and then transferred to nutrient medium with or without Fe for 24 hours. Expression levels were normalized to ubiquitin 10 (UBQ10) and then to the value of each gene from the Wt under Fe-sufficient conditions. Values are means ± SD (n = 3). +, significant change vs +Fe； *, significant change vs WT + Fe at $P <0.05$ (one-way-ANOVA).

Figure 4. Grouping of identified target proteins according to functional categories. Pie chart of all 117 identified target proteins grouped according to functional categories (Table S1).

Figure 5. Model depicting the effect of Fe deficiency on 14-3-3 interacting proteins with a role in ethylene biosynthesis and glycolysis. Fe deficiency induces ethylene production by up-regulating SAMS, ACS and ACO genes (in red); Fe deficiency increases the activity of GAPDH (in red) and down-regulates the phosphorylation level of CINV1 (in blue) in glycolysis pathway. Green symbol indicates the relationship is not clear between Fe deficiency and G6PD and HK. 14-3-3 proteins regulate the activity of many enzymes in these pathways through direct or indirect interaction. SAMS, S-adenosyl metionine synthetase; ACS, ACC synthase; ACO, ACC oxidase; ETO, ethylene-overproducer; CINV1, alkaline invertase1; HK, hexokinase; GAPDH, glyceraldehyde-phosphate dehydrogenase; G6PD, Glucose-6-phosphate 1-dehydrogenase.

Table 1. 14-3-3 Interactome changes in Wt and *klun* roots induced by Fe-deficiency. Interacting proteins were classified as Fe responsive when the ratio -Fe/+Fe was higher than 1.5 (increase in binding) or lower than 0.66 (decrease in binding) with a 95% confidence level ($P<0.05$, Students's t-test). Ratios were calculated from three biological replicates. Interactors are ranked according to functional categories. A ratio of zero implies that a protein found in the +Fe treatment was lost in the -Fe treatment.

Table 2. 14-3-3 Interactome differences between Wt and klun roots grown with sufficient Fe. Proteins with a ratio >1.5 are more abundant in the pull-down from Wt roots as compared to *klun*, whereas proteins with a ratio <0.66 are more abundant in the pull-down from *klun* roots as compared to Wt. Ratios were calculated from three biological replicates and only proteins with significant ratio difference are shown ($P<0.05$, Students's t-test).

Figures

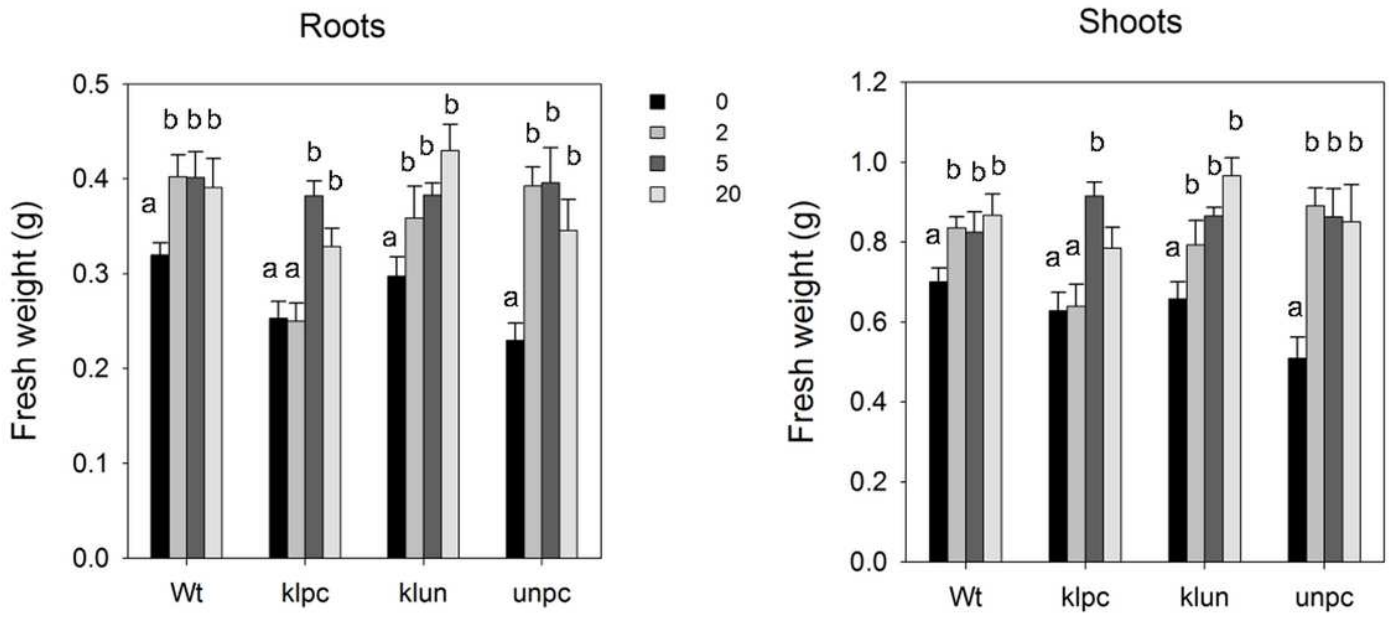

Figure 1

Growth performance of Wt and 14-3-3 qKOs under different Fe deficiency treatment. After two weeks of growth on ½ strength Hoagland solution, plants were grown for an additional 12 days at 0, 2, 5 and 20 µM (= sufficient) Fe. Fresh weight of roots (A), shoots (B) were measured from Wt and 14-3-3 qKOs plants. Each bar represents the mean of 10 biological replicates. The line above each bar is the SE. Means with different superscripts are significantly different at $P<0.05$, by two-way ANOVA followed by Bonferroni's post hoc test.

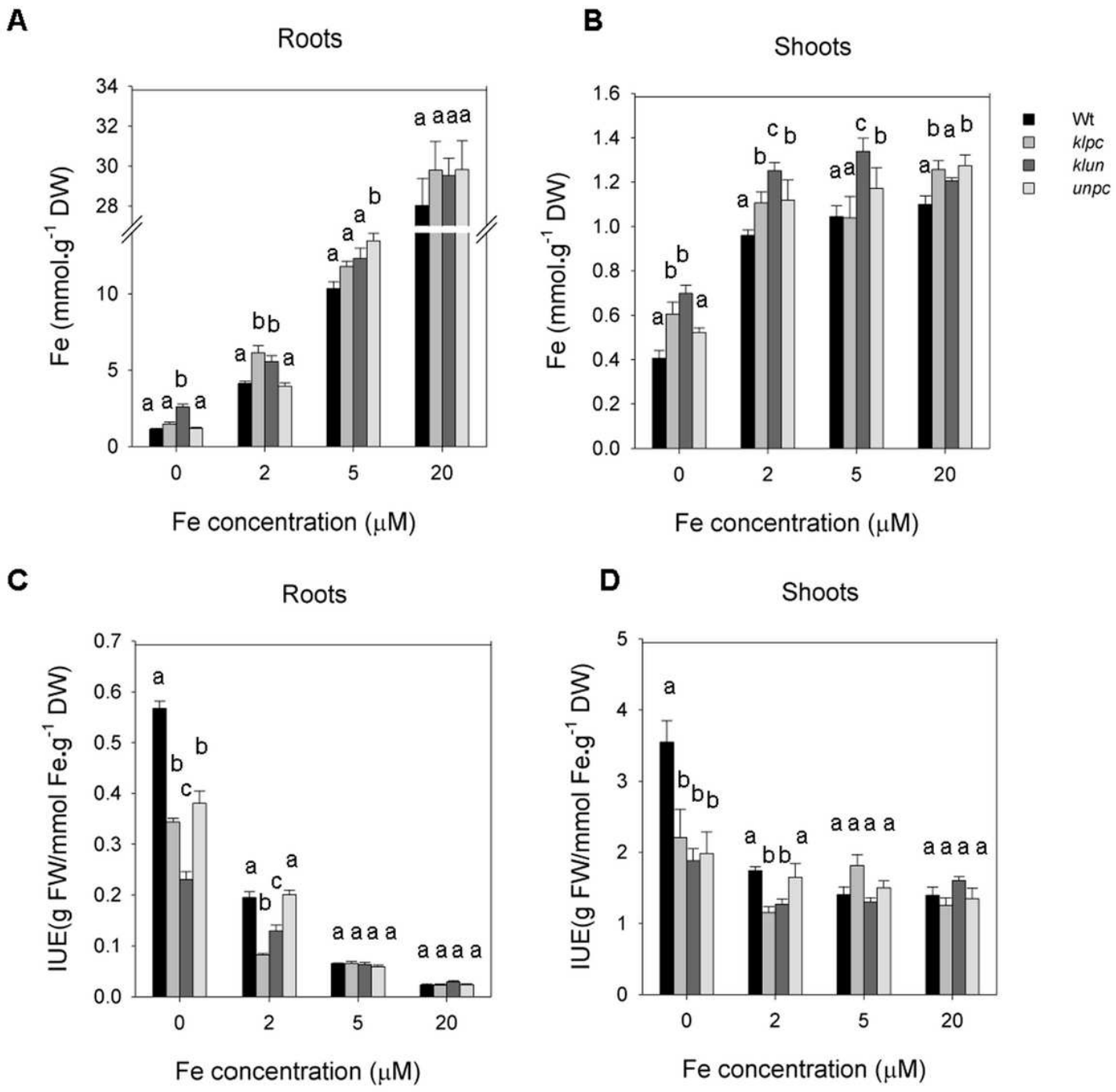

Figure 2

Fe content of shoots and roots of WT and 14-3-3 qKOs plants. After two weeks of growth on ½ strength Hoagland solution, plants were grown for an additional 12 days at 0, 2, 5 and 20 μM (= sufficient) Fe. Shoots and roots were harvested, weighed and pooled per two for the Fe-determination. A and B, Fe-content of roots and shoots; C and D, Iron Use Efficiency (IUE) of roots and shoots. Each bar represents a mean of observations in 5 biological replicates, ± SE. Averages with different superscripts are significantly different at $P<0.05$, by two-way ANOVA followed by Bonferroni's post hoc test.

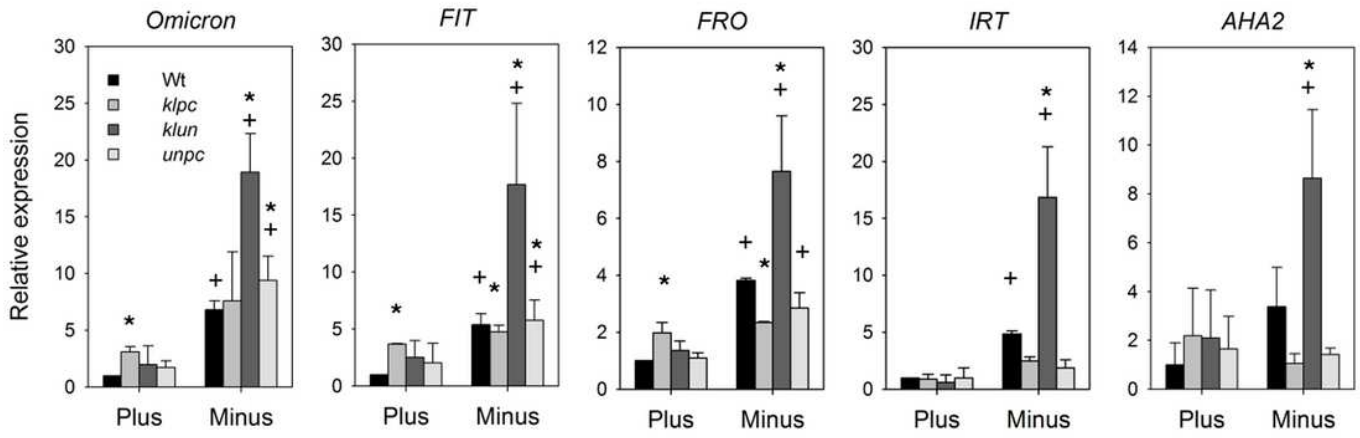

Figure 3

Expression analysis of 14-3-3 Omicron, FIT, FRO, IRT and AHA2 in Wt and 14-3-3 qKO lines grown with (plus) and without (minus) Fe. A. thaliana seedlings were grown in +Fe medium for 22 days and then transferred to nutrient medium with or without Fe for 24 hours. Expression levels were normalized to ubiquitin 10 (UBQ10) and then to the value of each gene from the Wt under Fe-sufficient conditions. Values are means ± SD (n = 3). +, significant change vs +Fe□*, significant change vs WT + Fe at P <0.05 (one-way-ANOVA).

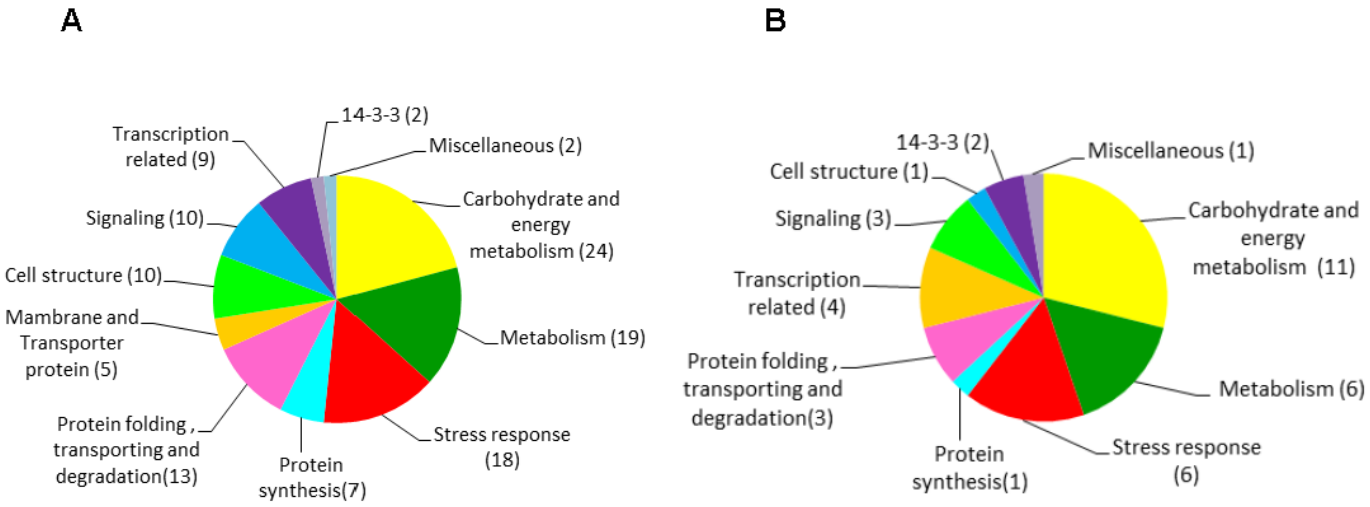

Figure 4

Grouping of identified target proteins according to functional categories. Pie chart of all 117 identified target proteins grouped according to functional categories (Table S1).

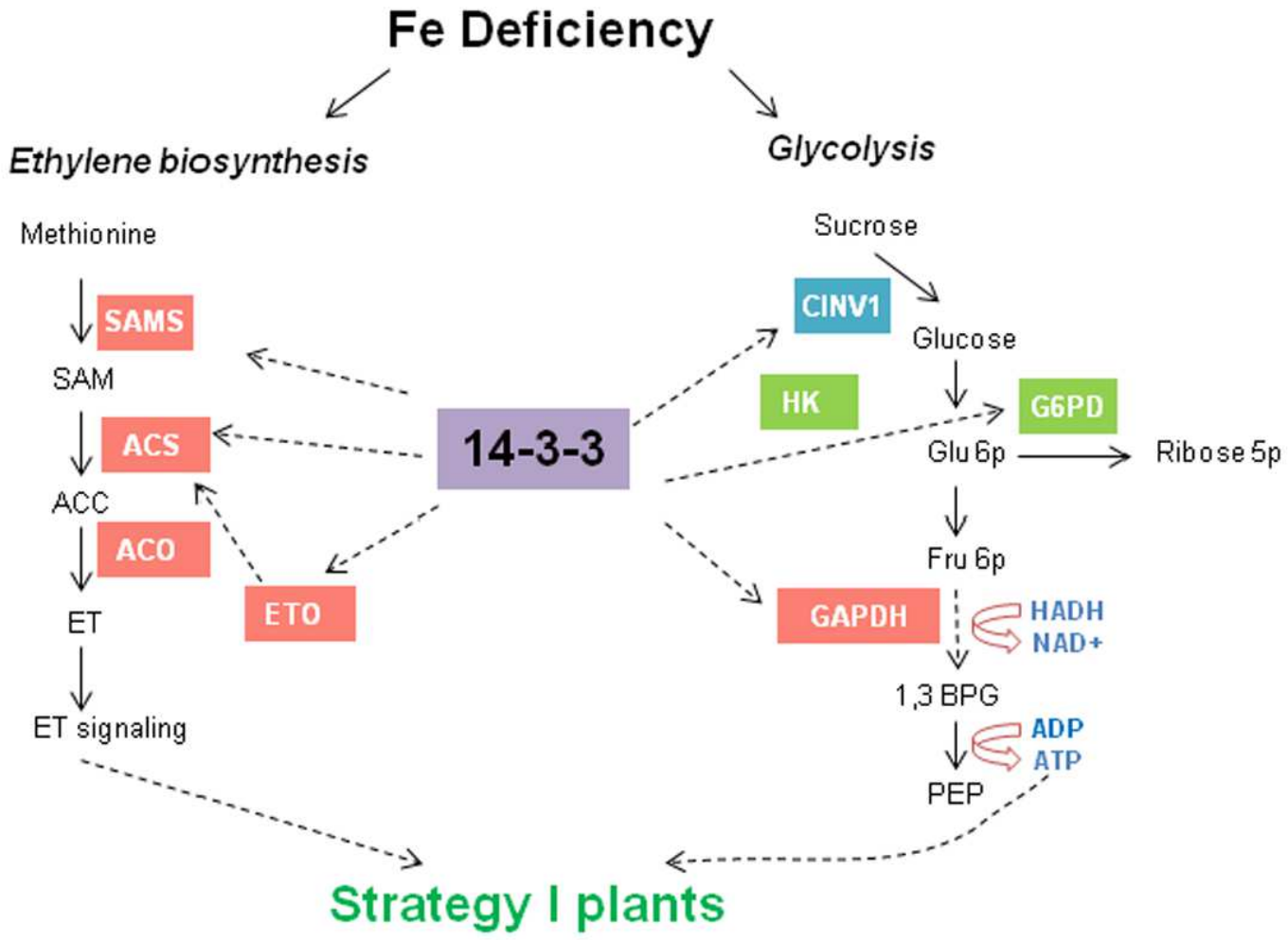

Figure 5

Model depicting the effect of Fe deficiency on 14-3-3 interacting proteins with a role in ethylene biosynthesis and glycolysis. Fe deficiency induces ethylene production by up-regulating SAMS, ACS and ACO genes (in red); Fe deficiency increases the activity of GAPDH (in red) and down-regulates the phosphorylation level of CINV1 (in blue) in glycolysis pathway. Green symbol indicates the relationship is not clear between Fe deficiency and G6PD and HK. 14-3-3 proteins regulate the activity of many enzymes in these pathways through direct or indirect interaction. SAMS, S-adenosyl metionine synthetase; ACS, ACC synthase; ACO, ACC oxidase; ETO, ethylene281 overproducer; CINV1, alkaline invertase1; HK, hexokinase; GAPDH, glyceraldehyde282 phosphate dehydrogenase; G6PD, Glucose-6-phosphate 1-dehydrogenase.

Supplementary Files

This is a list of supplementary files associated with this preprint. Click to download.

- SupplementaryInformation.docx